



Heterogeneous expression of predictive biomarkers PD-L1 and TIGIT in non-mucinous lung adenocarcinoma and corresponding lymph node metastasis: A challenge for clinical biomarker testing

Tobias Kolb, Julian Benckendorff, Peter Möller, Thomas F.E. Barth*, Ralf B. Marienfeld*

From the Institute of Pathology, Ulm University, Albert-Einstein-Allee 23, Ulm D-89070, Germany



ARTICLE INFO

Keywords:

NSCLC
Immune checkpoint proteins
Tumor heterogeneity
PD-L1
TIGIT

ABSTRACT

The use of immune checkpoint inhibitors (ICI) targeting the PD-L1:PD1 interaction revolutionized tumor treatment by re-activating the anti-tumoral capacity of the immune system. Assessment of tumor mutational burden, microsatellite instability, or expression of the surface marker PD-L1 have been used to predict individual response to ICI therapy. However, the predicted response does not always correspond to the actual therapy outcome. We hypothesize that tumor heterogeneity might be a major cause of this inconsistency. In this respect we recently demonstrated that PD-L1 shows heterogeneous expression in the different growth patterns of non-small cell lung cancer (NSCLC) - lepidic, acinar, papillary, micropapillary and solid. Furthermore, additional inhibitory receptors, like T cell immunoglobulin and ITIM domain (TIGIT), appear to be heterogeneously expressed and affect the outcome of anti-PD-L1 treatment. Given this heterogeneity in the primary tumor, we set out to analyze the situation in corresponding lymph node metastases, since these are often used to obtain biopsy material for tumor diagnosis, staging and molecular analysis. Again, we observed heterogeneous expression of PD-1, PD-L1, TIGIT, Nectin-2 and PVR in relation to different regions and growth pattern distribution that varied between the primary tumor and their metastases. Together, our study underscores the complex situation regarding the heterogeneity of NSCLC samples and suggest that the analysis of a small biopsy from lymph node metastases may not be sufficient to ensure a reliable prediction of ICI therapy success.

Introduction

Lung cancer ranks first among the deadliest cancers worldwide, with an approximate survival rate of 15% within 5 years [1]. It is classified into non-small cell lung cancer (NSCLC) with 85% and small cell lung cancer (SCLC) with 15% of all cases. The most common subtype of NSCLC is non-mucinous adenocarcinoma, which according to the 2015 WHO classification can present with lepidic, acinar, papillary, micropapillary and solid histological growth patterns [2]. Increasing evidence suggests that each growth pattern reflects the biologic diversity of the individual tumor and is therefore associated with a different prognosis [2–4]. In the late tumor stages solid and micropapillary growth patterns are more common and more often associated with metastases. Lepidic and papillary growth patterns, on the other hand, predominate in the early stages of the disease and correlate with higher survival rate of the NSCLC patients [5].

Under physiological conditions immune surveillance prevents cancer development by destroying malignant cells. Occasionally, however, tumor cells evade immune surveillance by evolving various mechanisms

that allow them to interfere with immune cell function. For instance, by downregulating their cell surface major histocompatibility complex (MHC), they become less recognizable by tumor antigen specific T lymphocytes [5]. Furthermore, cancer cells frequently modify glycosylation of cell surface proteins that are normally involved in tissue repair to facilitate metastases [2]. Another example for escape mechanism is the initiation of inhibitory pathways by engaging inhibitory receptors expressed by lymphocytes. The most prominent examples of such inhibitory receptors are CTLA-4, B7-H4, VISTA, and PD-1 [6]. The Programmed cell death protein 1 (PD-1, CD274) plays a vital role in inhibiting the immune response and promoting self-tolerance [7]. It is expressed on activated T cells, natural killer (NK) cells, B lymphocytes, dendritic cells (DCs), macrophages, and most notably on tumor infiltrating lymphocytes (TILs). The interaction of PD-1 with its ligand PD-L1 mediates functional exhaustion of CD8⁺ T cells and causes a decreased proliferation, the release of cytokines and the secretion of cytolytic factors [8], thus, leading to an immune suppressing microenvironment.

Blocking these T cell immune checkpoints is an effective method for cancer treatment. Both, clinical trials and basic research, showed that

* Corresponding authors.

E-mail addresses: thomas.barth@uniklinik-ulm.de (T.F.E. Barth), ralf.marienfeld@uniklinik-ulm.de (R.B. Marienfeld).

blockade of PD-1/PD-L1 with monoclonal antibodies, like nivolumab (Opdivo, 2015) and pembrolizumab (Tecentrig, 2017), is efficient to restore the immune response against various tumor types, such as non-small-cell lung cancer (NSCLC), metastatic renal cell carcinoma (RCC), bladder cancer and Hodgkin's lymphoma [3,9]. The FDA approved both drugs for the treatment of melanoma and non-small cell lung cancer. However, there is a low response rate of 20% for NSCLC patients who received primary immunotherapy with PD-1/PD-L1 inhibitors [8]. One reason for this low response rate are resistance mechanisms, either primary resistance or acquired during therapy. One potential resistance mechanism is the presence of other inhibitory receptors, which might act on the immunosurveillance redundantly [10].

One of these inhibitory receptors that came into focus for immunotherapy in recent years is T cell immunoreceptor with Ig and ITIM domains (TIGIT). By binding to its ligands poliovirus receptor (PVR) or poliovirus receptor-related 2 (Nectin-2), TIGIT-mediated signalling negatively regulates T cell activation through multiple mechanisms. TIGIT is widely expressed on lymphocytes like activated T cells, memory T cells, cytokine-induced killer cells (CIKs), regulatory T cells, follicular T helper cells, and natural killer cells. Activation of this immune checkpoint not only leads to the release of cytokine IL-10 by dendritic cells and inhibition of DC maturation, but also to further inhibitory intrinsic effects of T cells through recruitment of the phosphatases SHIP1 and SHP2 [11]. Furthermore, binding of TIGIT with its ligand PVR was found to lead to attenuation of NK cytotoxicity, granule polarisation, and cytokine release [10]. The relevance of the TIGIT axis as resistance mechanism against PD-1/PD-L1 blockade is highlighted by the fact that co-blockade of TIGIT and PD-1 improves tumor infiltrating CD8+ T-cell function and expansion. Currently, 6 monoclonal antibodies targeting TIGIT are in clinical trials, either for use as monotherapy or in combination with CTLA-4 or PD-1/PD-L1 for the treatment of patients with advanced solid malignancies [12]. Together, these data underscore the importance of reliably predicting the expression of PD-1/PD-L1 and components of the TIGIT axis in tumor samples. The evaluation of IC expression in NSCLCs is complicated by the fact that often only small tumor samples from lymph node metastases are available. Regarding the heterogenous expression of the PD-L1 and the TIGIT axis in primary tumors, we set out to clarify whether this heterogeneity is reflected in the lymph node biopsies used for diagnostic procedure.

Although immune checkpoint blockade has significantly improved clinical outcome, the prognostic relevance of expressed immune checkpoints in lymph node metastasis currently remains unknown. To reveal differences in IC expression between primary tumor and metastases, we compared the expression of the PD-1 and TIGIT axis of the metastases with previously published expression in the primary tumor with regard to the different histological growth patterns [10].

Material & methods

Cohort and patient description

In our previous study we included 22 patients with lung adenocarcinoma who were treated surgically at the medical Ulm hospital [10]. Of the 22 patients enrolled in the previous study, 11 patients with lymph node metastases were included. These corresponding lymph nodes were processed into 50 formalin-fixed paraffin-embedded (FFPE) tissue blocks and stored at the Institute of Pathology of the University Medical Centre Ulm. All samples were reviewed by two experienced pathologists before use. This study was approved by the Ethics Committee of the University of Ulm (ethic code 180/19), and performed in accordance with the declaration of Helsinki.

Immunohistochemical procedure

The expression levels of PD-1/PD-L1 and TIGIT/PVR/Nectin-2 were evaluated by immunohistochemistry (IHC). 2 µm-thick tissue sections

cut from FFPE blocks were placed on slides, deparaffinized in xylene for 5 min and rehydrated by incubation in decreasing ethanol concentrations for 5 min each. Different treatments for each antibody were used for the retrieval of the antigene. The tissue slides were either placed in a steamer (PD-L1, Nectin-2) or in a microwave (PVR, PD1 and TIGIT) with different buffer solutions, e.g., EDTA buffer pH 9.0 (PD-L1, Nectin-2), citrate buffer pH 6.0 (PD-1, PVR) or TRIS-based buffer pH 9.0 (TIGIT) for 20 min. The incubation with the primary antibody was performed for 30 min at room temperature (PD-L1, Nectin-2, PVR, PD-1) or overnight for at least 16h at 4°C (TIGIT). Subsequently, the Dako REAL detection system (Dako, Santa Clara, USA) and the Vectastain Elite Kit (Vector Laboratories, Burlingame, USA) were used according to manufacturer's instructions. Further, the slides were counterstained with hematoxylin, mounted and cover slipped.

Antibodies

The following antibodies were used: monoclonal antibody against PD-L1 (Quartett, Berlin, Germany, 1:200, QR1), PD-1 (Dianova, Hamburg, Germany, 1:50, JAD1), Nectin-2 (Cell Signaling, Danvers, USA, 1:50, D8D3F), PVR (Cell Signaling, Danvers, USA, 1:50, D8A5G), and TIGIT (Dianova, Hamburg, Germany, 1:25, TG1).

Pathohistological evaluation

Two experienced pathologists determined and recorded the histological growth patterns on a H.E. section. This was done under blind conditions. Of note, the histological growth patterns were evaluated separately for the immunohistopathological examinations. Tonsil and placental tissue were stained along with the lymph node metastases slides as positive and negative controls.

For the correct evaluation and comparability of the immunohistochemically stained slides we used the H-score for evaluation. Here, the tumor proportion score (TPS) is multiplied by the intensity of the staining, with 1 for a weak, 2 for an intermediate and 3 for a strong staining, leading to a H score range from 0 to 300.

Statistical analysis

The Mann-Whitney-U-Test and Spearman Correlation was used for statistical analyses of protein expression levels between the histological subtypes in primary lung tumor and metastasis. The values were considered statistically significant with a p-value of ≤ 0.05 . Pearson correlation coefficient analyses was performed by using GraphPad Prism 9 software. Venn diagram was calculated using R package 'VennDiagram' (version 1.6.20).

Results

Patient characteristics

A total of 11 patients were enrolled in this study. These patients are a part of a NSCLC cohort already analysed in a previous study, for which the expression level of different immune checkpoint proteins were determined in the primary tumor. All patients were diagnosed with NSCLC, graded between stage I-III, and contained metastases in the lymph nodes. The tumor samples were resected and collected at the University Medical Centre Ulm. The cohort included 3 male and 8 female patients with a median age of 64 years (range 48-79 years). Staging was performed according to the IASLC UICC TNM (8th edition) classification (Table 1).

46 FFPE blocks were derived from the primary tumors of these 11 patients, with the maximal number of 8 blocks for one tumor. For the lymph node metastases 50 FFPE blocks were derived, again with the

Table 1
Baseline characteristics of patient cohort.

primary tumor	lymph node metastasis	age at diagnosis	gender	grading	TNM-classification
Patient 1	-	42	f	I	pT1a, pNx, M0, L0, V0, R0
Patient 2	X	48	f	II-III	pT2a, pN2 (10/12), Mx, L1, R1
Patient 3	X	48	f	II	pT3, pN1 (1/41), Mx, V1, Rx
Patient 4	X	54	f	I-II	pT2b, pN2 (N1 3/4; N2 3/15) M1a, R0
Patient 5	X	54	f	II-III	pT2b, pN1 (7/7), Mx, L1, V1, R0
Patient 6	-	58	f	II	pT3, N0, M1b, L0, V0, Pn0, Rx
Patient 7	-	59	m	II	pT2a, pN0, M0, R0,
Patient 8	X	60	m	II	pT4, pN2, (N1 2/6; N2 17/34), Mx, L1, V0, V1, Pn0, R0
Patient 9	X	59	f	III	pT2a, pN2 (N1 2/5; N2 2/11), Mx, L0, V1, Pn0, R0
Patient 10	-	60	m	II	pT2, pN0 (0/7), Mx, L0, V0, V1, Pn0, R0
Patient 11	X	60	m	III	pT2a, pN2 (N1 2/9; N2 3/5), Mx, L1, V0, R0
Patient 12	X	62	m	I	pT1a, pN1 (8/11), Mx, L0, V0, R0
Patient 13	-	64	m	II	pT4, V0, L0, pN0 (N1 0/13; N2 0/15), Mx, R0
Patient 14	-	67	m	II	pT1b, V0, L0, N0 (0/2), Mx, R0
Patient 15	-	66	m	I-II	pT1b, V0, L0, N1 (N1 1/4, N2 0/3), Mx, R0
Patient 17	X	74	f	II	pT1b, pN2 (N1 4/6; N2 2/3), Mx, L0, V1, Pn0, R0
Patient 18	-	75	f	II	pT3, pN0 (0/18), Mx, L0, V0, Pn0, R1
Patient 19	X	74	f	I	pT2a, pN2 (7/28), M0, L0, V0, R0
Patient 20	-	77	f	III	pT1b, pN0, M0, R0
Patient 21	-	78	f	I-II	pT2, pNx, Mx, L0, V1, pN0, Rx
Patient 22	X	79	f	II	pT4, pN2 (N1 4/4; N2 9/23), M1a, R0

Table 2
Patients with number of infected lymph nodes and growth pattern distribution between primary tumor and metastasis.

Patient number	lymph node status	affected lymph nodes	Growth patterns primary tumor/block	Growth patterns metastasis/block
Patient 2 LN	N2(10/12)	10	(a)(a)(a,s)(a,s)	(p)(s)(s)(a)(a)(s)(p)(s)
Patient 3 LN	N1(1/41)	1	(a)	(s)
Patient 4 LN	N2(3/4 N1, 3/15 N2)	6	(l,a)(a,p)(a,p,s)(l,a,p,s)(l,a,p,s)	(s)(N.A)(s,a)(s,a)(s)
Patient 5 LN	N2(7/7)	7	(a)(a,s)(a,s)(a,p,s)	(s)(p,s)
Patient 8 LN	N2 (N1 2/6, N2 17/34)	19	(a,s,mp),(p,s,mp)(a,p,s)(a,p,mp)(a)(a)(a)	(s)(s)(s)(s)(p)(s,a)(s)
Patient 9 LN	N2 (N1 2/5, N2 2/11)	4	(l,s)(s)	(N.A)(s)(s)
Patient 11 LN	N2 (N1 2/9, N2 3/5)	5	(l,a,s)(l,a,s)	(s)(p)(s)
Patient 12 LN	N1 (8/11)	8	(a,mp)(a,p,s,mp)(a,p,mp)(a,p,s)	(s)(s)(s,a)(a)
Patient 17 LN	N2 (N1 4/6, N2 2/3)	6	(a,s)(a,s)(a,s)(a,s)(s)	(p)(p)(p)(s,a)(p)
Patient 19 LN	N2 (7/28)	7	(l,a)(l,a)(l,a)(l,a)	(s)(p)(s)
Patient 22 LN	N2 (N1 4/4, 9/23 N2)	13	(a,p,s,mp)(a,s,mp)	(s,a)(s)(s)(p)(s)(s)(a)(p)

bracket ≙ FFPE block, l=lepidic, a=acinar, p=papillary, mp=micropapillary, s=solid, N.A=not available

maximal number of one tumor with 8 FFPE blocks. By contrast, one patient had only 1 tumor block derived from the primary and the metastases, respectively, that could be examined. Subsequently, immunohistochemical and histopathological examination were carried out separately for each of the total 96 blocks.

Both, the 46 blocks of the primary tumor and 50 blocks of the metastases, were classified according to the World Health Organisation classification guidelines for lung cancer 2015 and categorized into different growth patterns.

In the primary tumor, up to 4 different growth patterns were identified in one FFPE block, in the metastases only up to 2 different growth patterns (Table 2). 95 different growth patterns were analyzed in the primary tumor, of which 24 were solid (25%), 12 papillary (13%), 42 acinar (44%), 9 micropapillary (9%), and 10 lepidic (11%). In the lymph node metastases, however, only 55 different growth patterns were determined, of which 33 were solid (60%), 12 papillary (22%), and 10 acinar (18%) (Fig. 1). The lepidic and micropapillary growth patterns were not observed in the lymph node metastases.

Almost all patients, except patient 3, showed at least two or more growth patterns in their primary tumor, whereas two patients (patient 3 and 9) harbored exclusively one growth pattern in their metastasis. Four patients showed exactly two growth patterns (patient 2, 9, 17, 19), one patient had 3 different growth patterns (patient 11), and 5 patients had 4 growth patterns (patient 4, 5, 8, 12, 22) in their primary tumor. However, in the metastatic sites five patients showed 2 distinct growth patterns (patient 4, 5, 9, 12, 19) whereas up to 3 different growth pat-

terns were found in the tumor samples of 4 patients (patient 2, 8, 17, 22).

Heterologous distribution of immune checkpoint proteins in lymph node metastases

The infiltrated lymph nodes were stained with antibodies against the immune checkpoint proteins PD-1, PD-L1, TIGIT, Nectin-2, and PVR and the H-score of the tumor tissue was then determined (Fig. 2 + 3). It was not possible to observe the tumor-infiltrating lymphocytes (TILs) in the lymph node metastasis specifically. Thus, it was not possible to determine the staining of TIGIT and PD-1 on the TILs in the metastases. Hence, we observed strong inter- and intratumoral heterogeneity for the expression of PD-1 and TIGIT in tumor tissue, as well as for their ligands PD-L1, PVR and Nectin-2 (Fig. 2 + 3). Moreover, immune checkpoint (IC) expression varied not only within the tumor, but also showed a substantial variation within a given growth pattern.

In lymph node metastases, we discovered several statistical differences in the expression of the IC proteins. We observed significantly higher expression of the TIGIT/PVR/Nectin-2 axis compared to the PD-1/PD-L1 axis. We found higher expression of TIGIT compared to PD-1 in all growth patterns present - acinar (p=0.0103), papillary (p=0.0009) and solid (p=0.0072) (Fig. 4).

By analyzing IC expression we found that TIGIT and Nectin-2 were expressed consistently regardless of the growth pattern (Fig. 4). In contrast, we found significantly higher PVR expression in regions with a

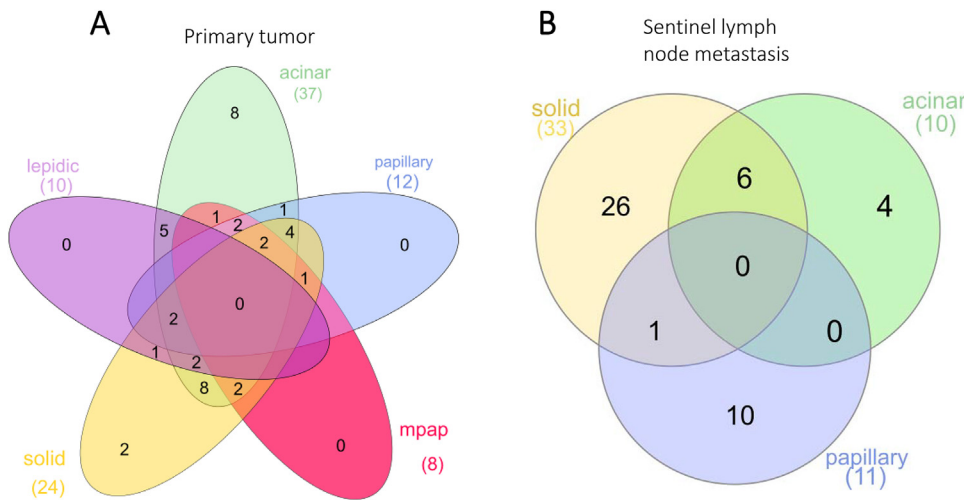


Fig. 1. Venn diagram of growth pattern distribution in primary tumor and metastasis. No micropapillary and lepidic growth pattern in metastasis. Ratio of growth pattern is different compared to primary tumor.

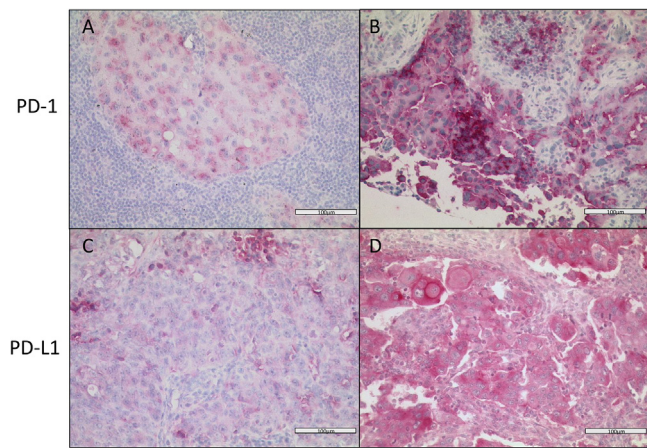


Fig. 2. Representative images of stained NSCLC lymph node metastasis sections with anti PD-1, PD-L1 antibodies. (A) An area of solid subtype with weak PD-1 staining of tumor cells and a H-Score of 80. (B) Strong staining of a solid tumor areal with anti-PD-1 antibodies. The H-Score is 300. (C) Weak expression of PD-L1 with an H-Score of 90 in a solid growth pattern. (D) Papillary growth pattern with strong staining against PD-L1. The H-Score was 280. Of note: first staining of tumor cells against PD-1 in NSCLC metastasis. All pictures were obtained in 20x magnification.

papillary growth pattern compared to regions with an acinar growth pattern (Suppl. Fig. 2B). PD-1 expression was only observed in acinar and solid growth pattern.

In regions with an acinar growth pattern PD-L1 expression was significantly lower than PD-1 expression in the acinar growth pattern ($p=0.0337$), but on an equal level in the solid and papillary growth pattern (Fig. 3).

Comparison of immune checkpoint expression between primary tumor and metastases

When comparing the expression level of these IC proteins in the metastases to those in the primary tumors, as we previously described [10], some clear differences become apparent. First, regions with a papillary growth pattern showed a significantly lower PD-1 expression in the metastases ($p=0.0103$) (Fig. 5B). Second, regions with a solid growth pattern showed a significantly lower PD-L1 expression in the metastases ($p=0.0031$) (Fig. 5C). Third, regions with an acinar growth pattern showed a significantly higher TIGIT expression in the metastases ($p=0.0202$) (Fig. 6A). Fourth, of the two ligands of TIGIT, only PVR

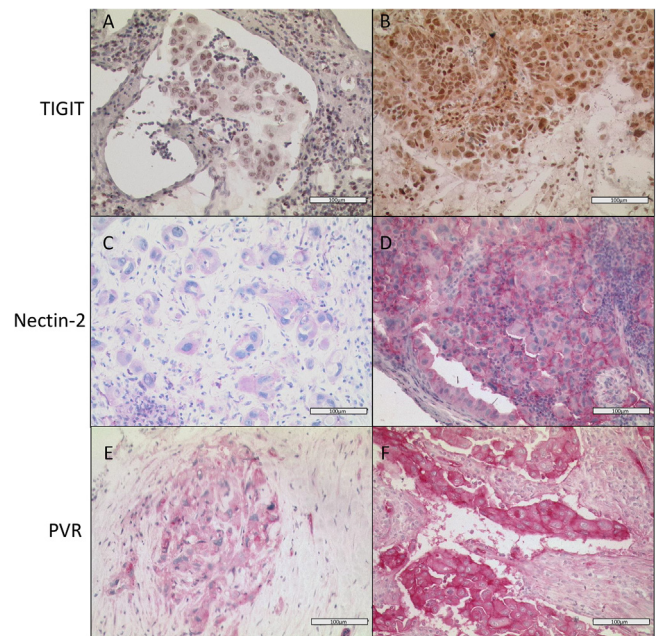


Fig. 3. Representative images of immunohistochemical staining with anti TIGIT, PVR, Nectin-2 antibodies. (A) Weak expression of TIGIT in tumor cells with a H-Score of 100. (B) Strong expression of TIGIT in tumor cells of solid growth pattern. Here the H-Score is 270. (C) Weakly anti-Nectin-2 staining of solid growing tumor cells with a H-Score of 100 (D) Strong positive anti-Nectin-2 staining of acinar and solid growing tumor cells with a H-Score of 220 (E) An area of papillary subtype weak positive for PVR. (F) A strong positive staining for PVR antibodies is depicted on all tumour cells in an acinar growth pattern. The H- Scores for both PVR stainings were 80 and 290. Of note: first staining of tumor cells against TIGIT in NSCLC metastasis. All pictures were obtained in 20x magnification.

showed a significantly lower/higher (?) expression in the solid and papillary growth pattern in the metastases (Fig. 6B, $p=0.0016$; $p=0.0283$), while Nectin-2 expression remained unchanged (Fig. 6C).

Regarding the distribution of immune checkpoint positive tumor areas (TPS), we again observed a high variability. This variability was both detectable in the metastatic sites, as well as in the primary tumor. For instance, PD-1 positive areas in the metastatic sites were more common in the acinar (19.4%) and solid (15.5%) subtype than in the papillary growth pattern (2.5%). Whereas, in the primary tumor, we observed

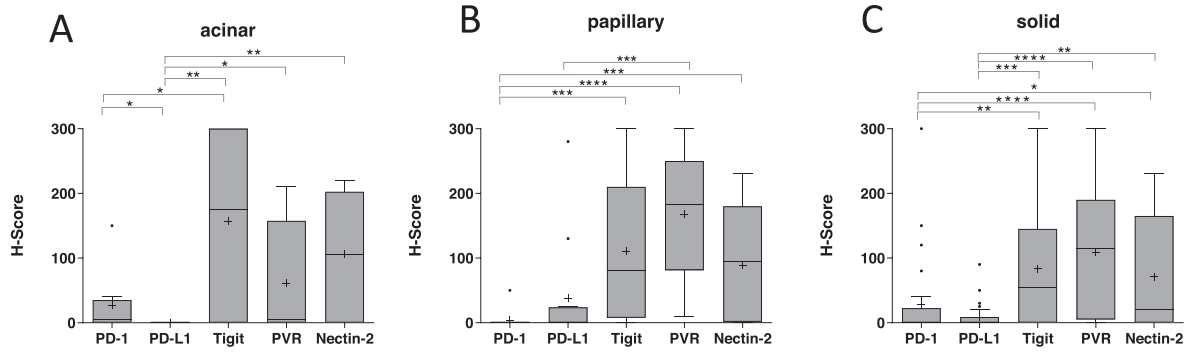


Fig. 4. Immune Checkpoints show a high diversity in expression in different growth patterns of NSCLC metastasis. Expression of different immune checkpoints in (A) acinar, (B) papillary, and (C) solid growth patterns assessed using H-Score. Mean values and standard deviation are shown. Statistical significance: *= $p \leq 0.05$, **= $p \leq 0.01$, ***= $p \leq 0.001$, ****= $p \leq 0.0001$.

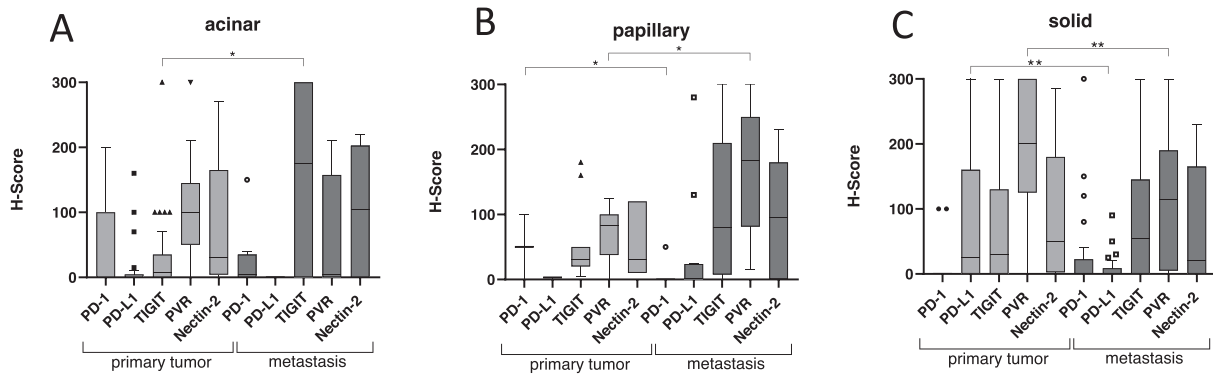


Fig. 5. Comparison of immune checkpoint expression between primary tumor and corresponding lymph node metastasis. Expression of different immune checkpoints in (A) acinar, (B) papillary, and (C) solid growth patterns assessed using H-Score. Mean values and standard deviation are shown. Statistical significance: *= $p \leq 0.05$, **= $p \leq 0.01$.

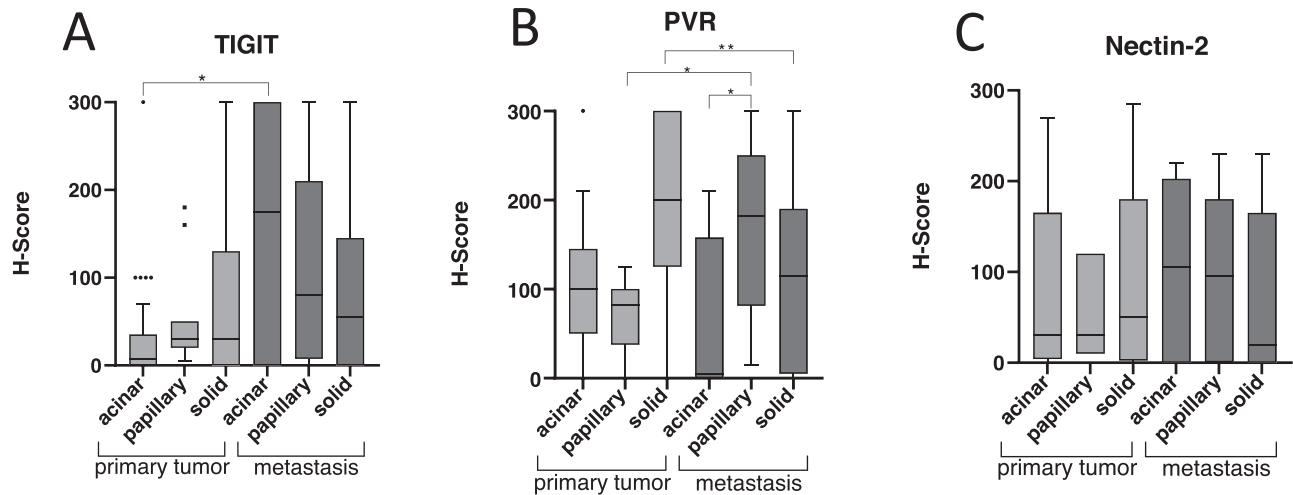


Fig. 6. Comparison of Immune checkpoint expression in different growth patterns compared to primary tumor. Comparison of immune checkpoints (A) TIGIT, (B) PVR, and (C) Nectin-2. Mean values and standard deviation are shown. Statistical significance: *= $p \leq 0.05$, **= $p \leq 0.01$, ****= $p \leq 0.0001$.

least positive areas of PD-1 in the acinar subtype (34.4%) (Suppl. Fig. 1).

Intra-individual variation of immune marker expression

Since we reported in our previous study a co-occurrence of the different immune checkpoint proteins in the primary tumor of NSCLC patients, we performed a similar analysis with the metastatic sites (Fig. 7).

The expression of the components of the TIGIT axis (TIGIT, PVR, Nectin-2) appears to be very heterogeneous and independent within the patients. Here, most of the patients expressed these immune markers in the tumor cells of the metastasis. Only patients 3 and 19 displayed no TIGIT expression at all. In a sharp contrast to the TIGIT axis, we detected no expression of the immune marker PD-1 and its ligand PD-L1 on the tumor cells of the metastatic sites in the majority of the patients (patients 2, 5, 8, 11, 17, 19 for PD-1(55 %); patients 2, 4, 5, 8,12 for PD-

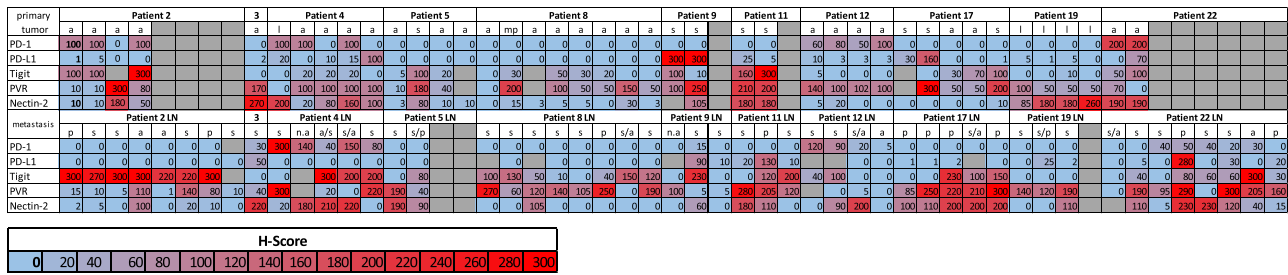


Fig. 7. Immune checkpoint protein expression in different growth patterns of each patient in both tumor sites. H-Scores are given for each patient sample.

L1(45 %)). However, most of these patients showed also no expression of PD-1 and PD-L1 in the primary tumor tissue. In general, the expression of the PD-1 axis was lower in the metastases than in the primary tumor. In addition, the expression of PD-1 and PD-L1 on tumor cells appeared not to be linked.

To explore potential correlations between the expression levels of the different analysed markers, we performed a Pearson correlation analysis. When considering the entire tumor, several correlations became apparent. PVR expression, for instance, showed a weak positive correlation with PD-1 ($r=0.292$; $p=0.038$) and a weak negative correlation with TIGIT expression ($r=-0.276$; $p=0.045$) (Fig. 8A). However, when we analysed the potential correlations in the growth patterns individually, we observed a different picture. For instance, a weak positive correlation of PVR with PD-1 was observed in the solid growth pattern ($r=0.370$; $p=0.044$) (Fig. 8D). Moreover, a very strong positive correlation of PD-1 and PD-L1 ($r=0.900$; $p=0.00007$) and a strong positive correlation of PVR and Nectin-2 was seen in the papillary growth pattern ($r=0.610$; $p=0.035$) (Fig. 8B). By contrast, no significant correlations for the analysed immune markers were found in the acinar growth pattern (Fig. 8A).

Similar expression of TIGIT axis components in N1 and N2 lymph node metastases

The pulmonary lymph nodes (N1) are usually the first lymph nodes to be metastatically involved in NSCLC, while only in a few cases the more distant mediastinal lymph nodes (N2) are also affected. To investigate a potential localisation-dependent change in immune checkpoint protein expression on tumor cells of N1 and N2 lymph node metastases, we compared the expression of the TIGIT/Nectin-2;PVR immune checkpoint proteins in the different N1 and N2 lymph node groups (Suppl. 6). Yet, no significant differences in these lymph node areas for either TIGIT or its two ligands were found.

Discussion

Main targets for immune checkpoint therapy in NSCLC are PD-1 and PD-L1 [13]. However, the response rate of patients remains at only 20 % [14,15]. One discussed reason for this low success rate is the heterogeneous expression of the PD-L1 in the tumor sample currently used as a predictive marker for PD-L1 immune therapy. Thus, heterogeneity of PD-L1 expression might lead to a PD-L1 under- or overestimation and therefore to false positive or false negative therapy prediction since characterization of a given NSCLC is often performed on basis of small biopsies that might not be representative for the tumor [16]. Moreover, as these biopsies are usually taken from the metastatic sites, we aimed to extend our previous findings by comparing the expression of various immune checkpoint proteins of the PD-1 and TIGIT axes between the primary tumor and its metastases. The relevance of this comparison is underlined by differences in protein levels of PD-1 and PD-L1, which varied significantly within and between individual growth patterns of a given metastasis. For example, we detected PD-L1 expression

in the papillary growth pattern areas at very low levels in the primary tumor whereas the metastatic site revealed higher PD-L1 expression levels. This is contradictory to previous reports in which the genomic and proteomic landscape of each growth pattern was determined in various types of cancers [17–19]. Brahmer et al. compared the PD-L1 expression of LUADs with non-paired metastases and observed a high expression of PD-L1 in both primary tumor and metastases [14,20]. The difference to our study may be due examination of LUADs with paired lymph node metastases of the same patients.

Besides the heterogeneous expression of PD-L1, the expression of additional immune checkpoint proteins with redundant functions is another potential resistance mechanism hampering the success of PD-L1 immune therapy. Therefore, it is important to compare the distribution of other immune checkpoint proteins, like T cell immunoglobulin and ITIM domain (TIGIT), with the already extensively studied PD-L1 expression. TIGIT is, like PD-1, an inhibitory receptor on CD8 positive T cells and is currently one of the most interesting immune markers for clinical research. In our previous study, we observed differences in the expression level of TIGIT in the primary tumor [17]. Here, we show that TIGIT and its ligands are expressed at similar levels in all growth patterns of the metastatic sites (Fig. 4). This was not expected, as we previously detected highly heterogeneous expression patterns of the very same immune checkpoint proteins in the primary tumor [21]. PVR, one of the ligands of TIGIT, was shown to be more expressed in the solid, papillary, and micropapillary growth patterns than in the lepidic and acinar growth patterns. We only saw significantly higher expression of PVR in the papillary growth pattern of the metastases (Fig. S1). We demonstrate here that TIGIT, like PD-1, is generally conserved on tumor cells in the metastases, which is in line with our previous study demonstrating TIGIT expression on tumor cells in the primary tumor [21]. Jin and colleagues showed TIGIT expression in tumor cells, however, not in human but in murine cell lines [18]. To the best of our knowledge, our study is the first to demonstrate TIGIT and PD-1 expression on tumor cells of metastatic sites.

In our previously work, we found a positive correlation of PVR and Nectin-2 with PD-1 in distinct growth patterns. Now, our current study revealed certain, growth pattern specific correlations of the expression of different components of the PD-1/PD-L1 and TIGIT/PVR/Nectin-2 axis determined by Pearson correlation analyses (Fig. 8). For instance, we saw a very strong correlation of PD-1 and PD-L1 as well as a strong correlation of PD-1 with PVR and Nectin-2 in the papillary growth pattern ($p=0.00007$ and $p= 0.035$, respectively). In contrast, these correlations were not seen in acinar growth pattern, but here, a strong correlation of PD-1 with TIGIT and Nectin-2 emerged. These differences in the correlations might further complicate the prediction of the success of a future combination therapy of PD-1/PD-L1 blockade with an interference with other immune checkpoints like TIGIT/Nectin-2 or PVR.

Tumor heterogeneity is represented by the growth patterns aforementioned. These may vary according to tumor stage and therefore correlate with prognosis. Grading systems have been established based solely on histological patterns in NSCLC [5,22,23]. Different subtypes may co-exist within a single tumor population; consequently, the tumor

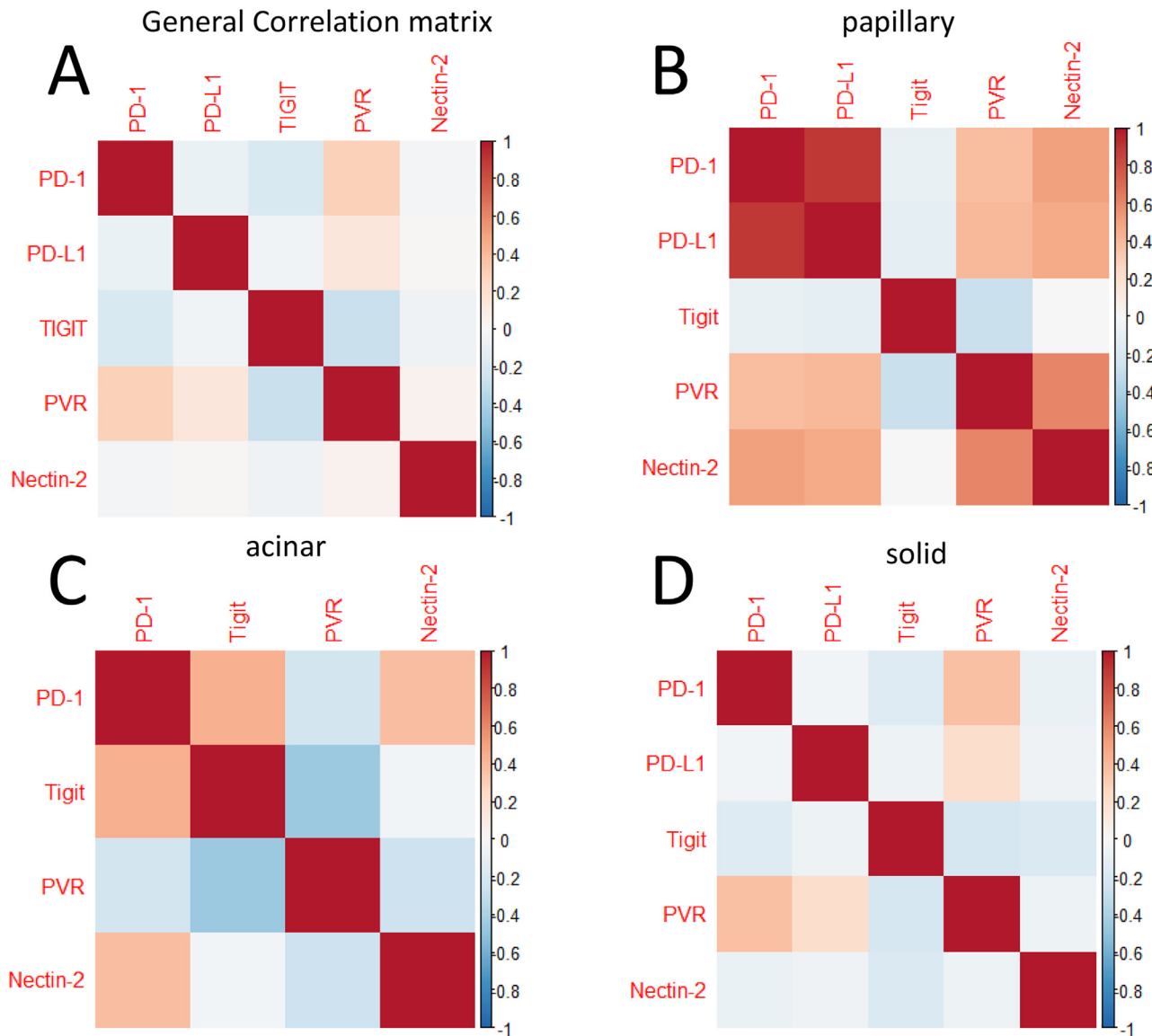


Fig. 8. Correlation of protein expression within different growth patterns. (A) Correlation of immune checkpoints in all metastasized sites. (B) Correlation of immune checkpoint proteins in papillary growth patterns. (C) Correlation of immune checkpoints in acinar growth patterns. (D) Correlation of immune checkpoints in solid growth pattern. Positive correlation is depicted with red colour, negative correlation with blue colour.

is classified by the predominant growth pattern, with reporting of the percentage of all the other identifiable patterns in 5% increments. This heterogeneity in the primary tumor poses therefore a major problem for successful therapy finding. In our study, we were able to show intratumoral heterogeneity due to multiple growth patterns detected within a lymph node metastasis. However, we saw a smaller variety of growth patterns in the metastases as compared to the primary tumor (Fig. 1). While the solid growth pattern was frequently observed, lepidic and micropapillary growth patterns were not present in the metastases. This is partially in line with previously published studies. Sica et al. found a lack of lepidic growth pattern in the metastatic sites, whereas the micropapillary growth pattern remained the predominant growth pattern in both the primary tumor and their corresponding lymph node metastasis [5]. Moreover, the ratio of growth patterns between the primary and the metastasized tumor is not fixed, as we observed independent changes of the growth patterns within several patients.

According to our study, the prediction of an immune checkpoint blockade, either targeting the PD-1/PD-L1 axis or the TIGIT/PVR/Nectin-2 axis, needs to be adjusted for the biomarker analysed, the given growth pattern, and the origin of the sample. However, as our study

was conducted with only 11 patients, additional large-scale studies are needed to further validate our findings.

In conclusion, our results highlight the inter- and intratumoral heterogeneity of lung adenocarcinoma and its corresponding lymph node metastasis. Moreover, our findings point to a challenge all personalized therapy approaches, which is that biopsies from small sites might not be sufficient to cover the entire molecular profile of the tumor. Since it is not possible to take several biopsies from each metastasis and analyse them in parallel, it is important to be aware that the analysis of one biopsy may not be reliably representative for the whole tumor. As a conclusion, our findings point to the question whether the results of the PD-L1 (or TIGIT/PVR) test should be used as a mandatory prediction tool at all.

Declaration of Competing Interest

The authors declare the following financial interests/personal relationships which may be considered as potential competing interests: We conceived financial support from Bristol-Myers-Squibb as part of a non-clinical research grant (OT123-391).

CRediT authorship contribution statement

Tobias Kolb: Investigation, Formal analysis, Writing – original draft. **Julian Benckendorff:** Investigation, Writing – review & editing. **Peter Möller:** Funding acquisition, Writing – review & editing. **Thomas F.E. Barth:** Conceptualization, Formal analysis, Supervision, Writing – review & editing. **Ralf B. Marienfeld:** Funding acquisition, Conceptualization, Supervision, Writing – review & editing.

Acknowledgement

We thank Frank Arnold for his help with the TIGIT staining and Michaela Häcker, Dilan Han and Marlene Schuster for excellent technical assistance. This work was supported by the German Research Foundation (DFG, GRK 2254 HEIST) and by a non-clinical research grant obtained from Bristol-Myers-Squibb (OT123-391).

Supplementary materials

Supplementary material associated with this article can be found, in the online version, at doi:[10.1016/j.neo.2023.100884](https://doi.org/10.1016/j.neo.2023.100884).

References

- [1] und R.L. Siegel, K.D. Miller, H.E. Fuchs, A. Jemal, "Cancer statistics, 2021", *CA Cancer J. Clin.* Bd. 71 (Nr. 1) (2021) 7–33. SJan., doi:[10.3322/caac.21654](https://doi.org/10.3322/caac.21654).
- [2] und M.B. Beasley, E. Brambilla, W.D. Travis, The 2004 World health organization classification of lung tumors, *Semin. Roentgenol.* 40 (Nr. 2) (2005) 90–97. Bd.SApr., doi:[10.1053/j.ro.2005.01.001](https://doi.org/10.1053/j.ro.2005.01.001).
- [3] und E. Kuhn, P. Morbini, A. Cancellieri, S. Damiani, A. Cavazza, C.E. Comin, *Adenocarcinoma classification: patterns and prognosis*, *Pathologica* 110 (Nr. 1) (2018) 5–11. Bd.SMärz.
- [4] und P.A. Russell, Z. Wainer, G.M. Wright, M. Daniels, M. Conron, R.A. Williams, Does lung adenocarcinoma subtype predict patient survival?: A clinicopathologic study based on the new international association for the study of lung cancer/American Thoracic Society/European respiratory society international multidisciplinary lung adenocarcinoma classification, *J. Thorac. Oncol.* 6 (Nr. 9) (2011) 1496–1504. Bd.SSep., doi:[10.1097/JTO.0b013e318221f701](https://doi.org/10.1097/JTO.0b013e318221f701).
- [5] G. Sica, A grading system of lung adenocarcinomas based on histologic pattern is predictive of disease recurrence in stage I tumors, *Am. J. Surg. Pathol.* 34 (Nr. 8) (2010) 1155–1162 Bd.SAug., doi:[10.1097/PAS.0b013e3181e4ee32](https://doi.org/10.1097/PAS.0b013e3181e4ee32).
- [6] und T. Azuma, S. Yao, G. Zhu, A.S. Flies, S.J. Flies, L. Chen, B7-H1 is a ubiquitous antiapoptotic receptor on cancer cells, *Blood* 111 (Nr. 7) (2008) 3635–3643. Bd.SApr., doi:[10.1182/blood-2007-11-123141](https://doi.org/10.1182/blood-2007-11-123141).
- [7] und G.P. Dunn, A.T. Bruce, H. Ikeda, L.J. Old, R.D. Schreiber, Cancer immunoediting: from immunosurveillance to tumor escape, *Nat. Immunol.* 3 (Nr. 11) (2002) 991–998. Bd.SNov., doi:[10.1038/ni1102-991](https://doi.org/10.1038/ni1102-991).
- [8] und Y. Han, D. Liu, L. Li, PD-1/PD-L1 pathway: current researches in cancer, *Am. J. Cancer Res.* 10 (Nr. 3) (2020) 727–742. Bd.SMärz.
- [9] und J. Crespo, H. Sun, T.H. Welling, Z. Tian, W. Zou, T cell anergy, exhaustion, senescence, and stemness in the tumor microenvironment, *Curr. Opin. Immunol.* 25 (Nr. 2) (2013) 214–221. Bd.SApr., doi:[10.1016/j.coi.2012.12.003](https://doi.org/10.1016/j.coi.2012.12.003).
- [10] und S. Müller, S. Mayer, P. Möller, T.F.E. Barth, R. Marienfeld, Spatial distribution of immune checkpoint proteins in histological subtypes of lung adenocarcinoma, *Neoplasia* 23 (Nr. 6) (2021) 584–593. Bd.SJuni, doi:[10.1016/j.neo.2021.05.005](https://doi.org/10.1016/j.neo.2021.05.005).
- [11] S.L. Topalian, Safety, activity, and immune correlates of Anti-PD-1 antibody in cancer, *N. Engl. J. Med.* 366 (Nr. 26) (2012) 2443–2454 Bd.SJuni, doi:[10.1056/NEJMoa1200690](https://doi.org/10.1056/NEJMoa1200690).
- [12] X. Yu, The surface protein TIGIT suppresses T cell activation by promoting the generation of mature immunoregulatory dendritic cells, *Nat. Immunol.* 10 (Nr. 1) (2009) 48–57 Bd.SJan., doi:[10.1038/ni.1674](https://doi.org/10.1038/ni.1674).
- [13] D. Planchard, Metastatic non-small cell lung cancer: ESMO clinical practice guidelines for diagnosis, treatment and follow-up, *Ann. Oncol.* 29 (Nr. Suppl 4) (2018) iv192–iv237 Bd.SOkt., doi:[10.1093/annonc/mdy275](https://doi.org/10.1093/annonc/mdy275).
- [14] J. Brahmer, Nivolumab versus docetaxel in advanced squamous-cell non-small-cell lung cancer, *N. Engl. J. Med.* 373 (Nr. 2) (2015) 123–135 Bd.SJuli, doi:[10.1056/NEJMoa1504627](https://doi.org/10.1056/NEJMoa1504627).
- [15] H. Borghaei, Nivolumab versus docetaxel in advanced nonsquamous non-small-cell lung cancer, *N. Engl. J. Med.* 373 (Nr. 17) (2015) 1627–1639 Bd.SOkt., doi:[10.1056/NEJMoa1507643](https://doi.org/10.1056/NEJMoa1507643).
- [16] M.J. Overman, Use of research biopsies in clinical trials: are risks and benefits adequately discussed? *J. Clin. Oncol.* 31 (Nr. 1) (2013) 17–22 Bd.SJan., doi:[10.1200/JCO.2012.43.1718](https://doi.org/10.1200/JCO.2012.43.1718).
- [17] D. Li, Genomic landscape of metastatic lung adenocarcinomas from large-scale clinical sequencing, *Neoplasia* 23 (Nr. 12) (2021) 1204–1212 Bd.SDez., doi:[10.1016/j.neo.2021.10.001](https://doi.org/10.1016/j.neo.2021.10.001).
- [18] X. Zhang, Differential expressions of PD-1, PD-L1 and PD-L2 between primary and metastatic sites in renal cell carcinoma, *BMC Cancer* 19 (Nr. 1) (2019) 360 Bd.SApr., doi:[10.1186/s12885-019-5578-4](https://doi.org/10.1186/s12885-019-5578-4).
- [19] E.Y. Kim, Genetic heterogeneity of actionable genes between primary and metastatic tumor in lung adenocarcinoma, *BMC Cancer* 16 (Nr. 1) (2016) 27 Bd.SJan., doi:[10.1186/s12885-016-2049-z](https://doi.org/10.1186/s12885-016-2049-z).
- [20] und H. Harjunpää, C. Guillerey, TIGIT as an emerging immune checkpoint, *Clin. Exp. Immunol.* 200 (Nr. 2) (2020) 108–119. Bd.SApr., doi:[10.1111/cei.13407](https://doi.org/10.1111/cei.13407).
- [21] N. Stanietsky, Mouse TIGIT inhibits NK-cell cytotoxicity upon interaction with PVRL2, *Eur. J. Immunol.* 43 (Nr. 8) (2013) 2138–2150 Bd.SAug., doi:[10.1002/eji.201243072](https://doi.org/10.1002/eji.201243072).
- [22] K. Kadota, A grading system combining architectural features and mitotic count predicts recurrence in stage I lung adenocarcinoma, *Mod Pathol* 25 (Nr. 8) (2012) 1117–1127 Bd.SAug., doi:[10.1038/modpathol.2012.58](https://doi.org/10.1038/modpathol.2012.58).
- [23] J.H. von der Thüsen, Prognostic significance of predominant histologic pattern and nuclear grade in resected adenocarcinoma of the lung: potential parameters for a grading system, *J. Thorac. Oncol.* 8 (Nr. 1) (2013) 37–44 Bd.SJan., doi:[10.1097/JTO.0b013e318276274e](https://doi.org/10.1097/JTO.0b013e318276274e).